

## Supplementary Information

### Magnetic Nanowire Networks for Dual-Isolation and Detection of Tumor-associated Circulating Biomarkers

HyungJae Lee<sup>1,4a</sup>, Mihye Choi<sup>1a</sup>, Jiyun Lim<sup>1</sup>, Minkyung Jo<sup>1,3</sup>, Ji-Youn Han<sup>2</sup>, Tae Min Kim<sup>5</sup>, and Youngnam Cho<sup>1,3\*</sup>

<sup>1</sup>Biomarker Branch, National Cancer Center, 323 Ilsan-ro, Ilsan-dong-gu, Goyang, Gyeonggi 10408, Korea

<sup>2</sup>Center for Lung Cancer, National Cancer Center, 323 Ilsan-ro, Ilsan-dong-gu, Goyang, Gyeonggi 10408, Korea

<sup>3</sup>Department of Cancer Biomedical Science, Graduate School of Cancer Science and Policy, 323 Ilsan-ro, Ilsan-dong-gu, Goyang, Gyeonggi 10408, Korea

<sup>4</sup>Department of Medical Science, Yonsei University College of Medicine, 50 Yonsei-Ro, Seodaemun-Gu, Seoul 03722, South Korea

<sup>5</sup>Department of Internal Medicine, Seoul National University Hospital, 101 Daehak-ro, Jongno-gu, Seoul 03080, Korea

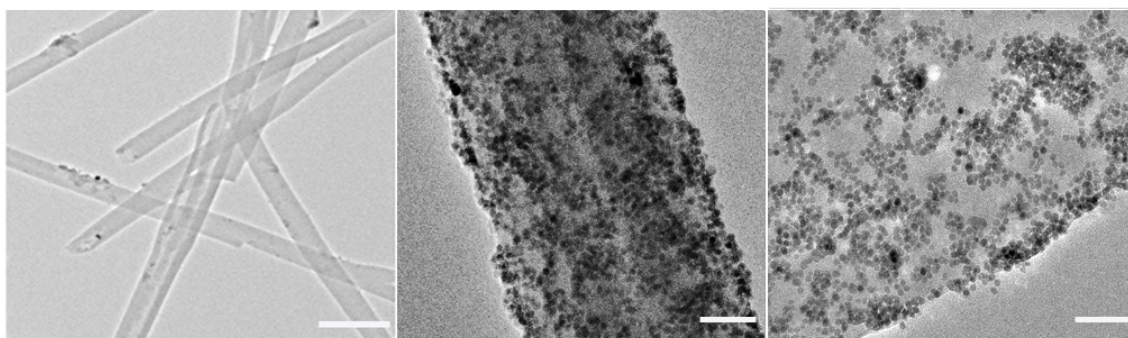
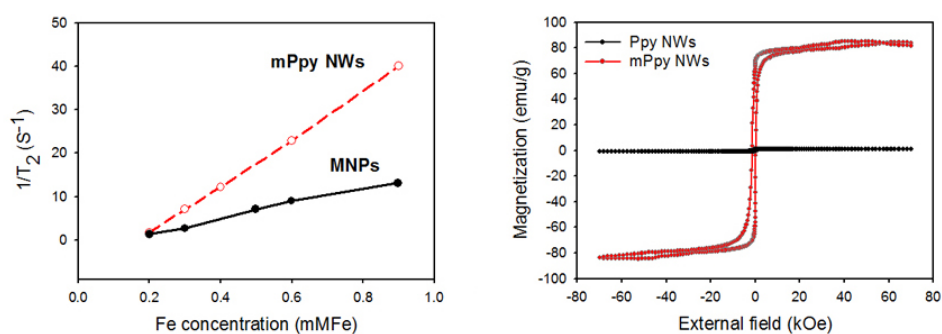
**A****B**

Figure S1. Characterization of *biotin-doped mPpy NWs*. (a) Left: transmission electron microscopic (TEM) images of the NWs (scale bar, 500 nm); middle and right: scanning electron microscopic (SEM) images of the NWs (scale bar, 50 nm). SEM and TEM images highlight the morphology of the NWs, whose average length was 18  $\mu\text{m}$  and diameter 200 nm, showing well-dispersed  $\text{Fe}_2\text{O}_3$  magnetic nanoparticles embedded in the inner surface of the mPpy NWs. (b) Transverse relaxation rates ( $1/T_2$ ,  $S^{-1}$ ) of magnetic NWs (mPpy NWs) and magnetic nanoparticles (MNPs) as a function of iron concentration (mMFe). (c) Magnetic hysteresis loop of magnetic NWs (mPpy NWs) and NWs (Ppy NWs) at room temperature.

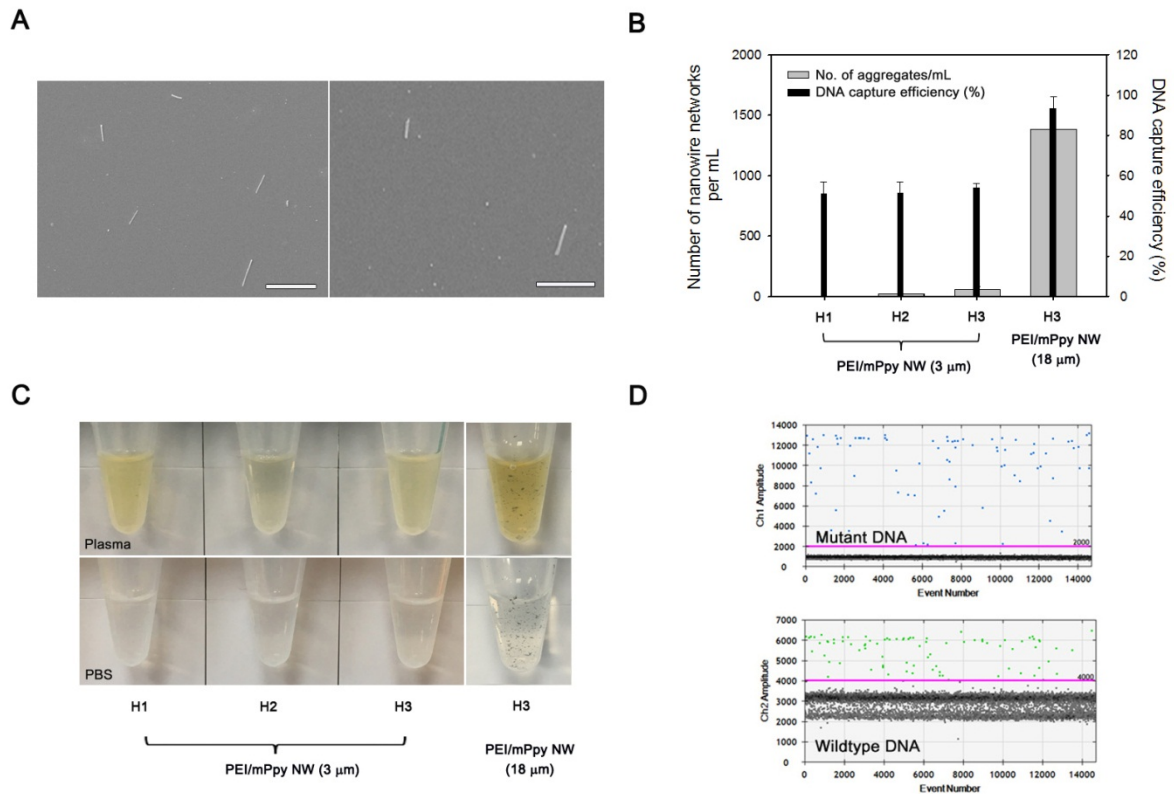


Figure S2. Effect of NW length on cfDNA extraction efficiency. (a) SEM images of NWs with an average length of 3  $\mu$ m and diameter of 200 nm (scale bar, 5  $\mu$ m). (b) Evaluation of the relationship between the amount of NW networks and DNA capture efficiency as a function of NW length, where DNA ladders (100 bp, 250 ng/mL) were spiked *ex vivo* into the plasma of three healthy donors. (c) The photographs confirm the presence of NW networks generated upon the addition of the NWs to plasma, where DNA ladders (100 bp, 250 ng/mL) were spiked *ex vivo* into the plasma of three healthy donors. Even after being transferred to PBS solution, the aggregates formed remained intact and were not dispersed. (d) Droplet digital PCR (ddPCR) confirmed that cfDNA extracted from the plasma of patients with lung cancer by using NWs of 18  $\mu$ m length has the same *EGFR* 19 mutation as tumor tissue. However, mutation status information could not be obtained from cfDNA extracted with NWs of 3- $\mu$ m length (data not shown).

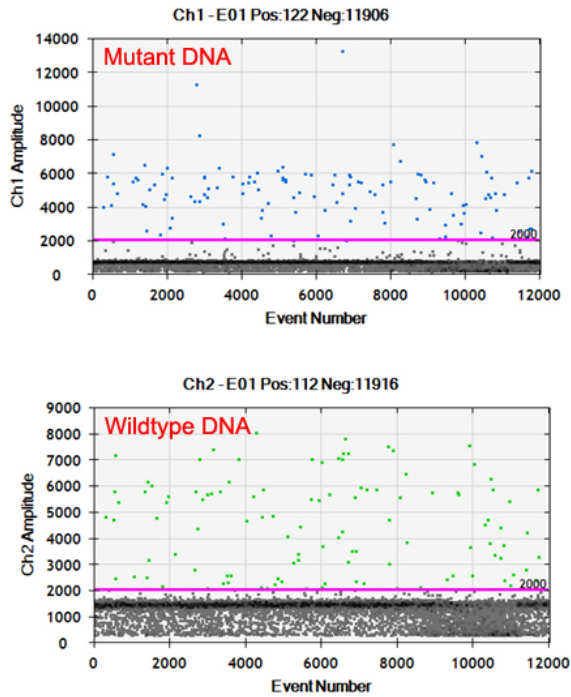
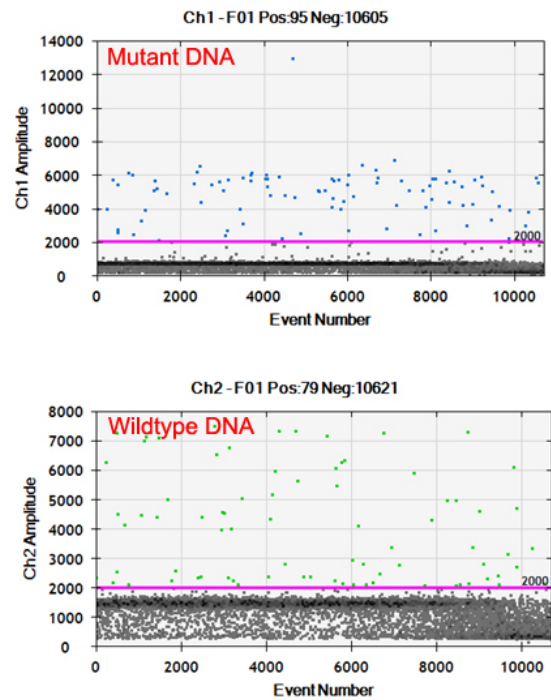
**A****cfDNA-nanowire conjugates****B****cfDNA released from nanowires**

Figure S3. Analysis of *EGFR* L858R mutation of cfDNA isolated from the plasma of a lung cancer patient by directly analyzing cfDNA-NW conjugates (left) and by releasing the DNA from the cfDNA-NW conjugates (right). ddPCR confirmed that both cfDNA in cfDNA-NW conjugates (left) and cfDNA released from the cfDNA-NW conjugates (right) harbor the same *EGFR* L858R mutation as tumor tissue.

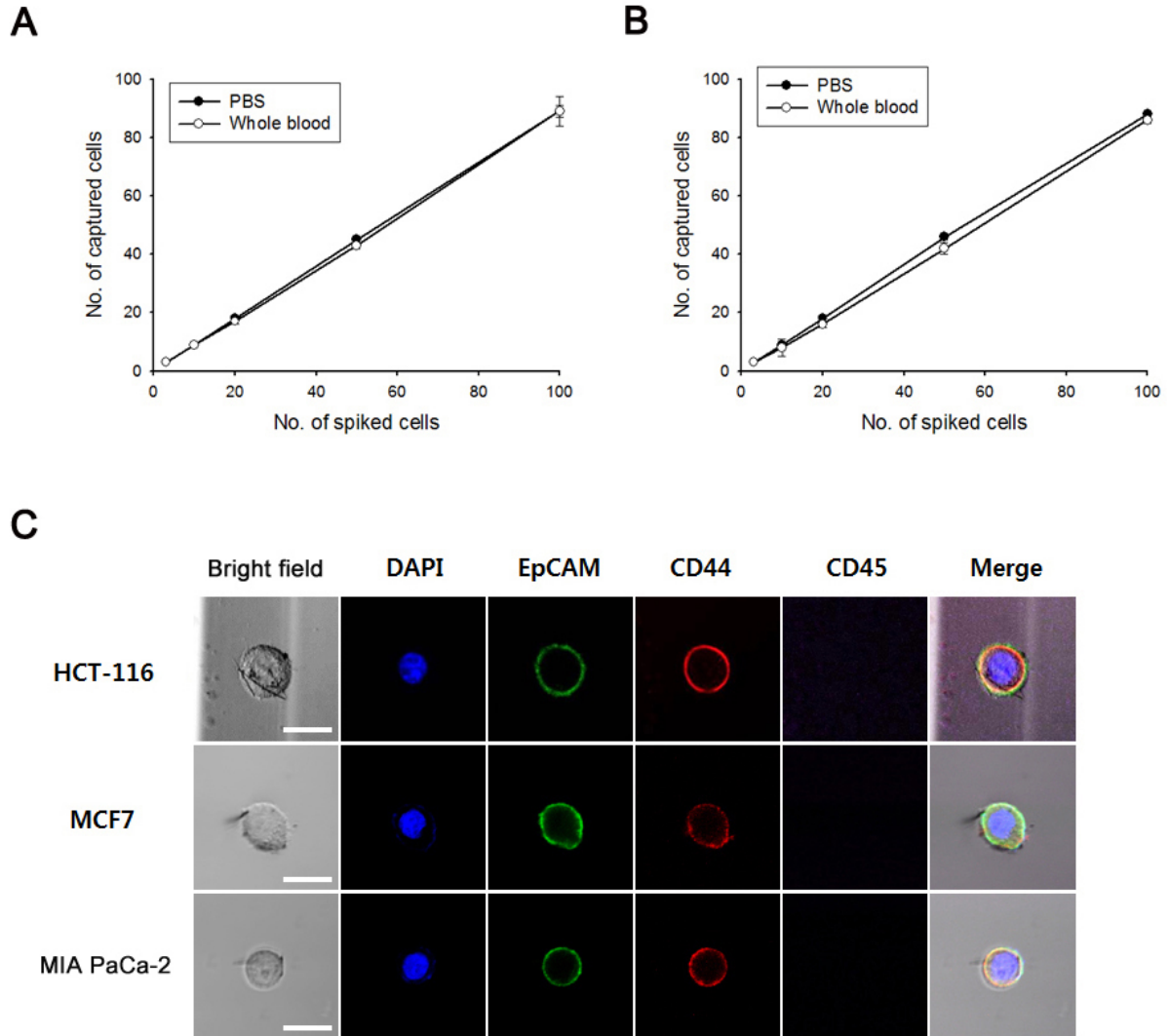


Figure S4. Examination of Ab cocktail/mPpy NWs using artificial blood samples. Quantitative evaluation of recovery efficiencies using artificial blood prepared by *ex vivo* spiking of (a) EpCAM-positive cells (MCF7 breast cancer) and (b) EpCAM-negative cells (MIA PaCa-2 pancreas cancer) into two different types of solution (PBS and whole blood). (c) Confocal images of cells captured from artificial blood samples and verified by four-color immunofluorescence staining (DNA (blue), CD45 (violet), EpCAM (green), and CD44 (red) (scale bar, 20  $\mu$ m).